Available online at www.derpharmachemica.com

Scholars Research Library

Der Pharma Chemica, 2015, 7(10):67-76
(http://derpharmachemica.com/archive.html)

ISSN 0975-413X
CODEN (USA): PCHHAX

Inhibition effects of a new syntheses pyrazole derivative on the corrosion of mild steel in sulfuric acid solution

S. EL Arouji[1], K. Alaoui Ismaili[1], A. Zerrouki[2], S. El Kadiri[2], Z. Rais[1], M. Filali Baba[1], M. Taleb[1], Khadijah M. Emran[3], A. Zarrouk[2], A. Aouniti[2] and B. Hammouti[2]

[1]Laboratoire d'Ingénierie d'Electrochimie de Modélisation et d'Environnement (LIEME) FSDM Fès, Morocco
[2]LCAE-URAC18, Faculty of Science, Mohammed first University, Oujda, Morocco
[3]Chemistry Department, Faculty of Science, Taibah University, Saudi Arabia

---

ABSTRACT

The corrosion inhibition of mild steel in 0.5 M H_2SO_4 in the presence of N^1,N^1-bis(2-(bis((3,5-dimethyl-1H-pyrazol-1-yl)methyl)amino)ethyl)-N^2,N^2-bis((3,5-dimethyl-1H-pyrazol-1- yl)methyl)ethane-1,2-diamine (PAP) has been studied by electrochemical techniques (DC polarization and AC impedance) and weight loss measurement. Result obtained reveal that this pyrazole derivative is good inhibitor for mild steel in 0.5 M H_2SO_4. Tafel polarization studies clearly reveal the type of inhibitor. This pyrazole derivative acts on cathodic and anodic reactions and reduces corrosion current density. Changes in impedance parameters (R_{ct} and C_{dl}) are indicative of adsorption of the pyrazole derivative on the metal surface leading to formation of protective film which grows with increasing concentration and inhibition efficiency values increase. The effect of temperature on the corrosion behavior of mild steel with the addition of the pyrazole derivative was studied in the temperature range from 303 to 333 K. Thermodynamic parameters for adsorption and activation processes were determined. Adsorption of this inhibitor follows the Langmuir adsorption isotherm.

Keywords: Mild steel, Pyrazole derivative, Adsorption, Electrochemical techniques, Weight loss measurement.

INTRODUCTION

Mild steel has found extensive application in various industries. Acidic solutions are used extensively in chemical and several industrial processes such as acid pickling, acid cleaning, acid descaling and oil wet cleaning and etc [1]. Chemical inhibitors are often used for these processes mainly to control the metal dissolution and acid consumption. Most of well known acid corrosion inhibitors are organic compounds containing nitrogen, sulfur or oxygen atoms. It has been found that most of the organic inhibitors act by adsorption on the metal surface [2-25]. This phenomenon is influenced by the nature and surface charge of metal, by the type of aggressive electrolyte, and by the chemical structure of inhibitors. Electrons transfer from inhibitor to the metal is facilitated when the inhibitor molecule has an unshared lone pair of electrons on the donor atom. Availability of π electron due to the presence of multiple bonds or aromatic rings in the inhibitor molecule would facilitate electron interact with d-orbital of iron [26, 27]. Some organic compounds have been synthesized and investigated as inhibitors for corrosion of metals in acidic solutions [28-31]. The objective of the present research paper was to study the inhibition action of newly synthesized pyrazole derivative on the corrosion of mild steel in 0.5 M H_2SO_4 at room temperature. The structure this pyrazole derivative is shown in Fig. 1.

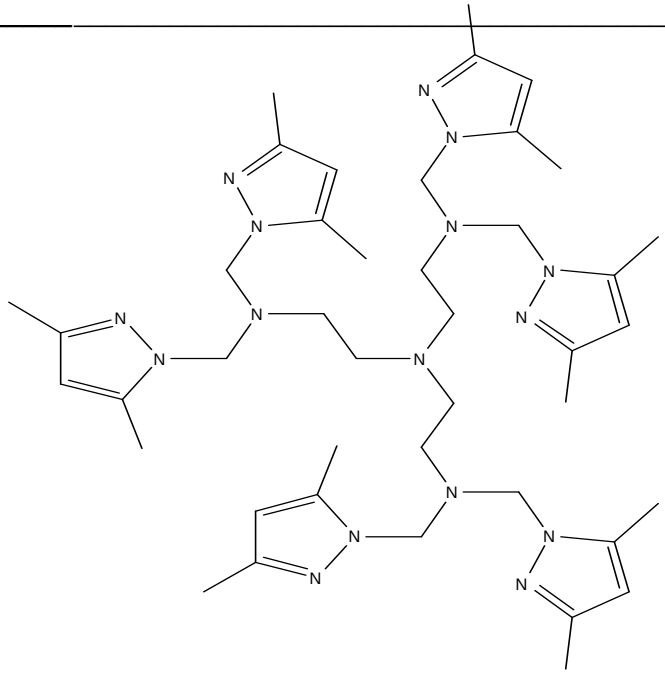

Figure 1: Molecular structure of the pyrazole derivative

MATERIALS AND METHODS

Materials

The steel used in this study is a mild steel with a chemical composition (in wt%) of 0.09%P, 0.01 % Al, 0.38 % Si, 0.05 % Mn, 0.21 % C, 0.05 % S and the remainder iron (Fe). The steel samples were pre-treated prior to the experiments by grinding with amery paper sic (220, 400, 800, 1000 and 1200); rinsed with distilled water, degreased in acetone, washed again with bidistilled water and then dried at room temperature before use.

Solutions

The aggressive solutions of 0.5 M H_2SO_4 were prepared by dilution of analytical grade 98% H_2SO_4 with distilled water. The concentration range of N^1,N^1-bis(2-(bis((3,5-dimethyl-1H-pyrazol-1-yl)methyl)amino)ethyl)-N^2,N^2-bis((3,5-dimethyl-1H-pyrazol-1- yl)methyl)ethane-1,2-diamine (PAP) used was 10^{-6}M to 10^{-3}M.

Gravimetric study

Gravimetric experiments were performed according to the standard methods [32], the mild steel sheets of 2 × 1 × 0.2 cm were abraded with a series of emery papers SiC (120, 600 and 1200) and then washed with distilled water and acetone. After weighing accurately, the specimens were immersed in a 50 mL beaker containing 100 mL of 0.5 M H_2SO_4 solution with and without addition of different concentrations inhibitor. All the aggressive acid solutions were open to air. After 6 h of acid immersion, the specimens were taken out, washed, dried, and weighed accurately. In order to get good reproducibility, all measurements were performed few times and average values were reported to obtain good reproducibility. The inhibition efficiency (η_{WL}%) and surface coverage (θ) were calculated as follows:

$$C_R = \frac{W_b - W_a}{At} \quad (1)$$

$$\eta_{WL}(\%) = \left(1 - \frac{w_i}{w_0}\right) \times 100 \quad (2)$$

$$\theta = \left(1 - \frac{w_i}{w_0}\right) \quad (3)$$

where W_b and W_a are the specimen weight before and after immersion in the tested solution, w_0 and w_i are the values of corrosion weight losses of mild steel in uninhibited and inhibited solutions, respectively, A the total area of the mild steel specimen (cm^2) and t is the exposure time (h).

Electrochemical measurements

The electrochemical measurements were carried out using Volta lab (Tacussel- Radiometer PGZ 100) potentiostate and controlled by Tacussel corrosion analysis software model (Voltamaster 4) at under static condition. The corrosion cell used had three electrodes. The reference electrode was a saturated calomel electrode (SCE). A platinum electrode was used as auxiliary electrode of surface area of 1 cm^2. The working electrode was mild steel of the surface 1 cm^2. All potentials given in this study were referred to this reference electrode. The working electrode was immersed in test solution for 30 min to a establish steady state open circuit potential (E_{ocp}). After measuring the E_{ocp}, the electrochemical measurements were performed. All electrochemical tests have been performed in aerated solutions at 298 K. The EIS experiments were conducted in the frequency range with high limit of 100 kHz and different low limit 0.1 Hz at open circuit potential, with 10 points per decade, at the rest potential, after 60 min of acid immersion, by applying 10 mV ac voltage peak-to-peak. Nyquist plots were made from these experiments. The best semicircle can be fit through the data points in the Nyquist plot using a non-linear least square fit so as to give the intersections with the *x*-axis.

The inhibition efficiency of the inhibitor was calculated from the charge transfer resistance values using the following equation:

$$\eta_z\% = \frac{R_{ct}^{i} - R_{ct}^{\circ}}{R_{ct}^{i}} \times 100 \qquad (4)$$

Where, R°_{ct} and R^{i}_{ct} are the charge transfer resistance in absence and in presence of inhibitor, respectively.

After ac impedance test, the potentiodynamic polarization measurements of mild steel substrate in inhibited and uninhibited solution were scanned from cathodic to the anodic direction, with a scan rate of 1 mV s^{-1}. The potentiodynamic data were analysed using the polarization VoltaMaster 4 software. The linear Tafel segments of anodic and cathodic curves were extrapolated to corrosion potential to obtain corrosion current densities (I_{corr}).
The inhibition efficiency was evaluated from the measured I_{corr} values using the following relationship:

$$\eta_{Tafel}(\%) = \frac{I_{corr} - I_{corr(i)}}{I_{corr}} \times 100 \qquad (5)$$

where I_{corr} and $I_{corr(i)}$ are the corrosion current densities for steel electrode in the uninhibited and inhibited solutions, respectively.

RESULTS AND DISCUSSION

Gravimetric study

Effect of concentration

The inhibition efficiency with different concentration of the inhibitor (PAP) on mild steel has been evaluated by weight loss measurements and the results are given in Table 1. In all cases, the value of η_{WL} increases with increase in inhibitor concentration, suggesting an increase of the number of molecules adsorbed on mild steel surface [33], blocking the active sites of acid attack which protects the metal from corrosion. The maximum efficiency of PAP is 94% in 0.5 M H_2SO_4. The corrosion inhibition of the compound is due to the presence of heteroatom (N) and serval cycles pyrazoles.

Table 1: Weight loss values of various concentrations of PAP in 0.5 M H_2SO_4 solution

Medium	Conc (M)	C_R (mg/cm^2 h)	θ	η_{WL} (%)
Blank	1.0	1.608	—	—
PAP	10^{-3}	0.097	0.94	94
	10^{-4}	0.129	0.92	92
	10^{-5}	0.289	0.82	82
	10^{-6}	0.322	0.80	80

Effect of Temperature

The effect of temperature on the performance of the PAP (Table 2) clearly indicates that the corrosion rate increases with increasing temperature. Adsorption and desorption of inhibitor molecules continuously occur at the metal surface and an equilibrium exists between two processes at a particular temperature. With increase of temperature,

the equilibrium between the adsorption and desorption processes is shited to a higher desorption rate than adsorption until equilibrium is again established at a different value of equilibrium constant.

Table 2: Weight loss values of PAP at 10^{-3} M at various temperatures in 0.5 M H_2SO_4 solution

Medium	Temp (K)	C_R (mg/cm^2 h)	θ	η_{WL} (%)
Blank	303	1.619	—	—
	313	3.862	—	—
	323	8.298	—	—
	333	14.407	—	—
PAP	303	0.162	0.90	90
	313	0.368	0.90	90
	323	1.649	0.80	80
	333	4.322	0.70	70

The activation thermodynamic parameters of the corrosion process were calculated from Arrhenius Eq. (6) and transition state Eq. (7) [34]:

$$C_R = k \exp\left(-\frac{E_a}{RT}\right) \quad (6)$$

$$C_R = \frac{RT}{Nh}\exp\left(\frac{\Delta S_a}{R}\right)\exp\left(-\frac{\Delta H_a}{RT}\right) \quad (7)$$

where E_a is the apparent activation corrosion energy, R is the universal gas constant, k is the Arrhenius pre-exponential factor, h is Plank's constant, N is Avogrado's number, ΔS_a is the entropy of activation and ΔH_a is the enthalpy of activation.

Figure 2 presents the Arrhenius plots of the natural logarithm of the corrosion rate vs. 1/T for mild steel in 0.5 M H_2SO_4 without and with addition of PAP. The calculated values of activation energy are given in Table 3. The data show that the activation energy (E_a) of the corrosion in mild steel in 0.5 M H_2SO_4 solution in the presence of this compound is higher than that in the free acid solution. The increase in the apparent activation energy for mild steel dissolution in inhibited solution may be interpreted as physical adsorption that occurs in the first stage [35]. Szauer and Brand explained [36] that the increase in activation energy can be attributed to an appreciable decrease in the adsorption of the inhibitor on the mild steel surface with increase in temperature.

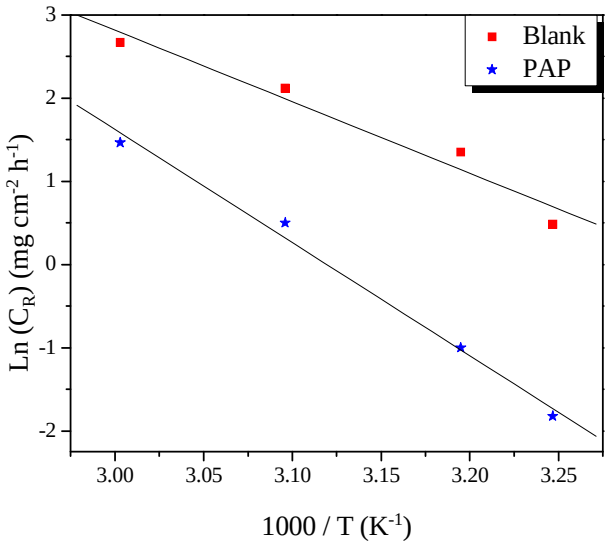

Figure 2: Arrhenius plots of Ln C_R vs. 1/T for mild steel in 0.5 M H_2SO_4 in the absence and the presence of PAP at optimum concentration

Figure 3 shows a plot of Ln (C_R/T) against 1/T. A straight lines are obtained with a slope of ($-\Delta H_a/R$) and an intercept of (Ln $R/Nh + \Delta S_a/R$) from which the values of ΔH_a and ΔS_a are calculated and are listed in

Table 3. Inspection of these data reveals that the ΔH_a value for dissolution reaction of mild steel in 0.5 M H_2SO_4 in the presence of PAP is higher than that of in the absence of inhibitor. The positive signs of ΔH_a reflect the endothermic nature of the mild steel dissolution process suggesting that the dissolution of mild steel is slow in the presence of inhibitor [37].

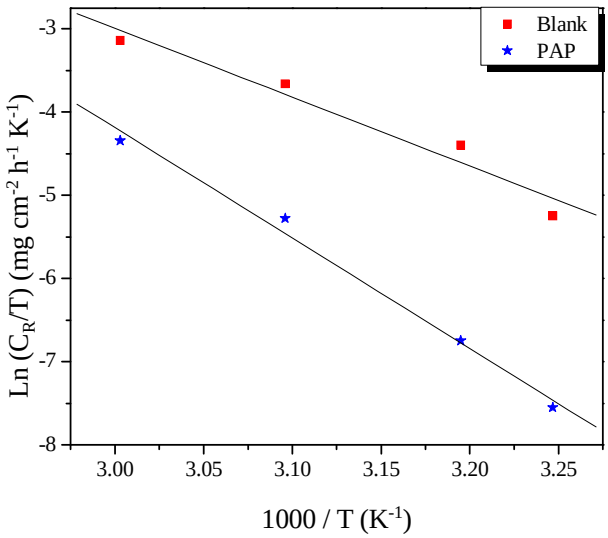

Figure 3: Arrhenius plots of Ln (C_R /T) vs. 1/T for mild steel in 0.5 M H_2SO_4 in the absence and the presence of PAP at optimum concentration

In addition, the value of ΔS_a was higher for inhibited solutions than that for the uninhibited solution (Table 3). This suggested that an increase in randomness occurred on going from reactants to the activated complex. Thus the increasing in entropy of activation was attributed to the increasing in solvent entropy [38].

Table 3: Corrosion kinetic parameters for mild steel in 0.5 M H_2SO_4 of PAP

Medium	*k* (mg cm^{-2} h^{-1})	E_a (kJ/mol)	ΔH_a (kJ/mol)	ΔS_a (J/mol K)
Blank	2.62×10^{12}	71.41	68.78	-16.06
PAP	2.57×10^{18}	112.94	110.33	98.64

Adsorption isotherm

The interactions between the inhibitor and the mild steel surface can be examined by the adsorption isotherm. The inhibition efficiency is directly proportional to the fraction of the surface covered by the adsorbed molecules (θ), which was calculated in this case using the equation $\theta = \eta_{WL}$ (%)/100. The adsorption isotherms most frequently used are Langmuir, Temkin, Frumkin and Flory-Huggins. Therefore, each of these adsorption isotherms was tested for its ability to describe the adsorption behavior of PAP on a mild steel surface in an H_2SO_4 solution. The coefficient of determination (R^2) was considered to choose the isotherm that best fitted the experimental data. The linear relationships of C/θ vs. C, shown in Figure 4, suggest that the adsorption of PAP on the mild steel obeyed the Langmuir adsorption isotherm. This isotherm can be represented as:

$$\frac{C}{\theta} = \frac{1}{K} + C \qquad (8)$$

where K is the adsorption constant, C is the concentration of the inhibitor and surface coverage values (θ) are obtained from the weight loss measurements for various concentrations. Plots of C/θ versus C yield a straight line as shown in Fig. 4. In this case the linear regression coefficient (R^2) is equal 1 and the slopes is very close to 1, indicating that the adsorption of PAP in 0.5 M H_2SO_4 follows the Langmuir isotherm and exhibit single-layer adsorption characteristic. According to Eq. 8, K can be calculated from intercept on the C/θ axis. By use of the equation below, ΔG°_{ads} can be calculated from K.

$$\Delta G^{\circ}_{ads} = -RTLn(55.5K_{ads}) \qquad (9)$$

Where R is gas constant and T is absolute temperature of experiment and the constant value of 55.5 is the concentration of water in solution in mol L^{-1}. The thermodynamics parameters derived from Langmuir adsorption isotherm for the studied compound, are given in Table 4.

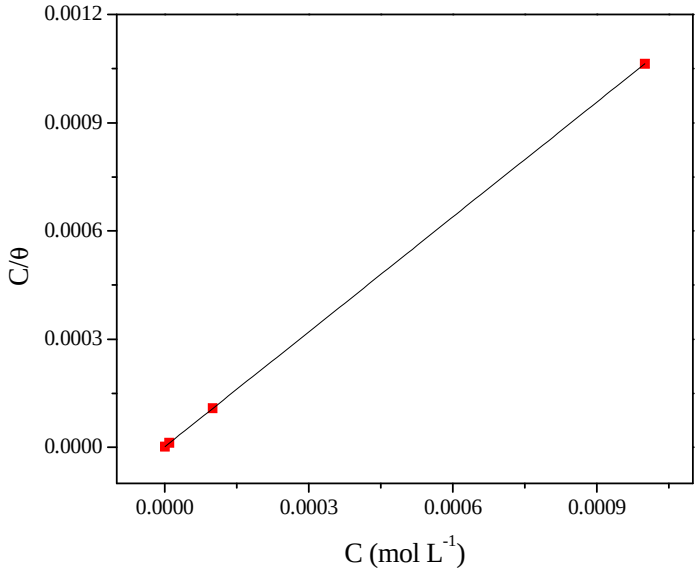

Figure 4: Langmuir adsorption of PAP on the mild steel surface in 0.5 M H_2SO_4 solution

Table 4: Thermodynamic parameters for the adsorption of PAP in 0.5 M H_2SO_4 on the mild steel at 298 K

Inhibitor	Slpoe	K (M^{-1})	R^2	ΔG°_{ads} (kJ/mol)
PAP	1.06	735158.98	1.0	-43.42

The values of ΔG°_{ads} was also listed in Table 4. The negative values of ΔG°_{ads} suggest that the adsorption of PAP is a spontaneous process. Generally speaking, values of ΔG°_{ads} up to -20 kJ mol^{-1} indicate the electrostatic attraction between the charged metal surface and charged organic molecules in the bulk of the solution (physisorption). Those around -40 kJ mol^{-1} or smaller involve charge sharing or charge transfer between the metal and the organic molecules (chemisorption) [39]. In the present study, the calculated standard free energy of adsorption value is closer to -40 kJ mol^{-1} (Table 4). Therefore it can be concluded that the adsorption of the PAP on the mild steel surface is more chemical than physical [40].

Potentiodynamic polarization study

In order to characterize the studied polymers as either anodic, cathodic, or mixed inhibitor for the corrosion process of mild steel in 0.5 M H2SO4 solutions, polarization experiments were undertaken. Typical anodic and cathodic curves obtained for the dissolution of mild steel in the acid induced environment without and with various concentrations of PAP at 298 K are depicted in Figure 5. In order to obtain information about the kinetics of the corrosion, some electrochemical parameters, i.e., corrosion potential (E_{corr}), corrosion current density (I_{corr}), cathodic tafel slopes (β_c) and the inhibition efficiency (η_{Tafel}) obtained from the polarization measurements were listed in Table 5.

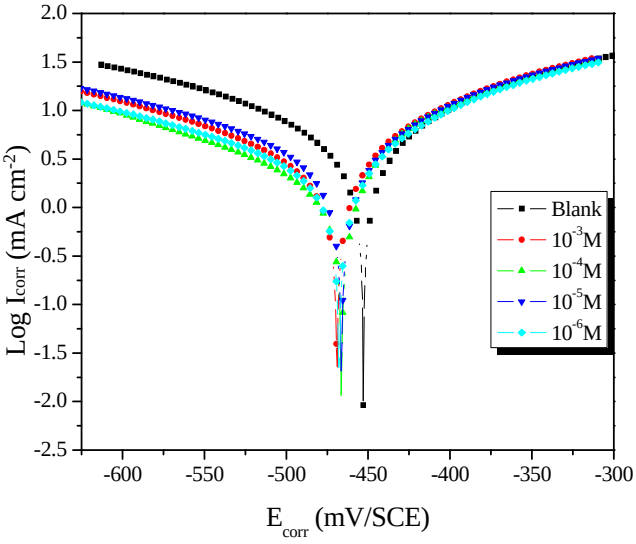

Figure 5: Polarization curves of mild steel in 0.5 M H_2SO_4 containing different concentrations of PAP

Table 5: The electrochemical parameters for mild steel in 0.5 M H_2SO_4 solution without and with different concentration of PAP at 298 K

Medium	Conc (M)	$-E_{corr}$ (mV/SCE)	$-\beta_c$ (mV dec^{-1})	I_{corr} (μA cm^{-2})	η_{Tafel} (%)
H_2SO_4	0.5	452.9	232.5	6861.6	—
PAP	10^{-3}	465.9	183.9	384.2	94
	10^{-4}	468.4	181.0	548.9	92
	10^{-5}	468.7	199.3	1578.1	77
	10^{-6}	452.9	193.8	1606.3	76

Inspection of Fig. 5 shows that the addition of PAP has an inhibitive effect in the both anodic and cathodic parts of the polarization curves and shifts both the anodic and cathodic curves to lower current densities. The reduction in I_{corr} is pronounced more and more with the increasing inhibitor concentration. It has been observed that 10^{-3} M of PAP serves as an optimum concentration that exhibit higher efficiency of corrosion inhibition. The increased inhibition efficiency with the inhibitor concentration indicates that the tested organic compound acts by adsorbing on the mild steel surface. The presence of PAP in 0.5 M H_2SO_4 solution shifts the corrosion potential slightly towards more negative potentials with respect to the corrosion potential observed in the unhibited solution. The largest displacement of E_{corr} was about 15.5 mV (< 85 mV), which indicates that PAP might act as a mixed-type inhibitor [41]. The cathodic branch of polarization curves was given rise to parallel lines. This shows that the addition of PAP to the 0.5 M H_2SO_4 solution does not change the cathodic hydrogen evolution mechanism and the decrease of H^+ ions on the surface of mild steel take place mainly through a charge transfer mechanism [42]. The inhibition effect of PAP may be caused by the simple blocking effect, namely the reduction of reaction area on the corroding surface.

Electrochemical impedance spectroscopy (EIS)

Electrochemical impedance spectroscopy is a veritable tool and has been widely used in investigating corrosion inhibition processes. It provides information on both the resistive and capacitive behaviour at an interface and makes it possible to evaluate the performance of test compounds as possible inhibitors against metal corrosion [43,44]. Fig. 6 illustrate the Nyquist of mild steel in 0.5 M H_2SO_4 solution without and with various concentrations of PAP at 298 K. It is seen that all the Nyquist plots for mild steel in test solutions consist of a capacitive loop at high frequencies (HF) and an inductive loop at low frequencies (LF), and the diameter of HF capacitive loop significantly enhances and the LF inductive loop gradually degrades as the inhibitor concentration increases, which indicate the presence of the inhibitor has little influence on the corrosion mechanism [45] and the corrosion process of mild steel in test solution is mainly charge-transfer controlled [46]. The HF capacitive loop is usually related to the time constant of charge transfer and double layer capacitance [45,47-49], while the LF inductive loop is attributed to the relaxation process obtained by adsorption species such as $(SO_4^{2-})_{ads}$ and $(H^+)_{ads}$ [46-49] or adsorption-desorption process of inhibitive molecules on working electrode surface [45,46]. Amin et al. think that the $(SO_4^{2-})_{ads}$ is most probable adsorption specie as the electrode surface has positive charges in the acid medium at the corrosion potential

[47]. The HF capacitive loops show depressed semicircle, which are attributed to the frequency dispersion due to the roughness and non-homogeneity of working electrode surface [50,51]. The impedance parameters namely, R_s, R_{ct}, C_{dl} and η, are given in Table 6.

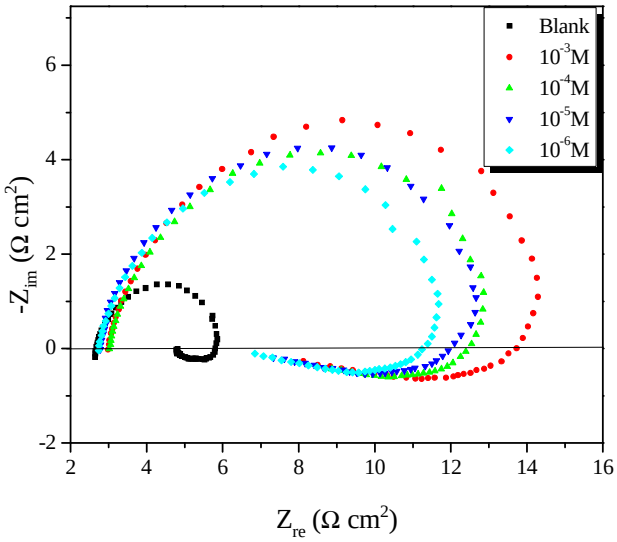

Figure 6: Nyquist plots for mild steel in 0.5 M H_2SO_4 solution without and with different concentration of PAP at 298 K

Table 6: Impedance parameters with corresponding inhibition efficiency for the corrosion of mild steel in 0.5 M H_2SO_4 at different concentrations of PAP

Medium	Conc (M)	R_s (Ω cm^2)	R_{ct} (Ω cm^2)	C_{dl} (μF cm^{-2})	η_z (%)
H_2SO_4	0.5	2.7	2.8	229.8	—
PAP	10^{-3}	3.0	49.2	102.5	94
	10^{-4}	3.0	31.3	102.4	91
	10^{-5}	2.7	14.6	110.0	81
	10^{-6}	2.7	14.1	142.3	80

The results in the Table 6 show that R_{ct} increased with increase in the concentration of PAP which also corresponds with the increase in the diameter of the semicircles, while C_{dl} decreased with increase in concentration. This behaviour could be related to the formation of an insulated adsorption layer [52], of PAP onto the steel surface leading to the formation of a film which isolates the metal from dissolution and charge transfer. In addition, the more the inhibitor is adsorbed, the greater the thickness of the barrier layer according to the Helmholtz model given in eqn (9) [53]:

$$C_{dl} = \frac{\varepsilon \varepsilon_0 A}{d} \qquad (10)$$

where d is the thickness of the protective layer, ε is the dielectric constant of the medium, ε_0 is the vacuum permittivity and A is the efective area of the electrode.

CONCLUSION

The following results can be drawn from this study:

✓PAP acts as a good inhibitor for the corrosion of mild steel in 0.5 M H_2SO_4 and its inhibition efficiency is concentration dependent.

✓The inhibition efficiencies could be increased with the increase of PAP concentration, but also be decreased by rising temperature.

✓The polarization measurements reveal that PAP behaves as a mixed-type inhibitor in 0.5 M H_2SO_4 by acting on both anodic metal dissolution and cathodic hydrogen evolution reactions.

✓The adsorption of the inhibitor on the surface of mild steel in 0.5 M H_2SO_4 follows a Langmuir adsorption isotherm. The high value of adsorption equilibrium constant and negative value of standard free energy of adsorption suggested that PAP is strongly adsorbed on mild steel surface

REFERENCES

[1] V.S. Sastri, *Corrosion Inhibitors*, N.Y.: John Wiley and Sons, **1998**.
[2] S. Kertit, B. Hammouti, *J. Appl. Electrochem.*, **1996**, 93, 59.
[3] L. Wang, *Corros. Sci.*, **2001**, 43, 1637.
[4] A.H. Al Hamzi, H. Zarrok, A. Zarrouk, R. Salghi, B. Hammouti, S.S. Al-Deyab, M. Bouachrine, A. Amine, F. Guenoun, *Int. J. Electrochem*. Sci., **2013**, 8, 2586.
[5] A. Zarrouk**,** B. Hammouti, H. Zarrok, I. Warad, M. Bouachrine, *Der Pharm. Chem*., **2011**, 3, 263.
[6] D. Ben Hmamou, R. Salghi, A. Zarrouk, M. Messali, H. Zarrok, M. Errami, B. Hammouti, Lh. Bazzi , A. Chakir, *Der Pharm. Chem*., **2012**, 4, 1496.
[7] A. Ghazoui, N. Bencaht, S.S. Al-Deyab, A. Zarrouk, B. Hammouti, M. Ramdani, M. Guenbour, *Int. J. Electrochem. Sci*., **2013**, 8, 2272.
[8] A. Zarrouk, H. Zarrok, R. Salghi, N. Bouroumane, B. Hammouti, S.S. Al-Deyab, R. Touzani, *Int. J. Electrochem. S*ci., **2012**, 7, 10215.
[9] H. Bendaha, A. Zarrouk, A. Aouniti, B. Hammouti, S. El Kadiri, R. Salghi, R. Touzani, *Phys. Chem. N*ews, **2012**, 64, 95.
[10] S. Rekkab, H. Zarrok, R. Salghi, A. Zarrouk**,** Lh. Bazzi, B. Hammouti, Z. Kabouche, R. Touzani, M. Zougagh, *J. Mater. Environ. Sci*., **2012**, 3, 613.
[11] A. Zarrouk, B. Hammouti, H. Zarrok, M. Bouachrine, K.F. Khaled, S.S. Al-Deyab, *Int. J. Electrochem. Sci.*, **2012**, 6, 89.
[12] A. Ghazoui, R. Saddik, N. Benchat, M. Guenbour, B. Hammouti, S.S. Al-Deyab, A. Zarrouk, *Int. J. Electrochem. Sci*., **2012**, 7, 7080.
[13] H. Zarrok, K. Al Mamari, A. Zarrouk, R. Salghi, B. Hammouti, S. S. Al-Deyab, E. M. Essassi, F. Bentiss, H. Oudda, *Int. J. Electrochem. Sci*., **2012**, 7, 10338.
[14] H. Zarrok, A. Zarrouk, R. Salghi, Y. Ramli, B. Hammouti, M. Assouag, E. M. Essassi, H. Oudda and M. Taleb, *J. Chem. Pharm. Res*., **2012**, 4, 5048.
[15] A. Zarrouk, B. Hammouti, A. Dafali, F. Bentiss, *Ind. Eng. Chem. Res.* **2013**, 52, 2560.
[16] H. Zarrok, A. Zarrouk, R. Salghi, H. Oudda, B. Hammouti, M. Assouag, M. Taleb, M. Ebn Touhami, M. Bouachrine, S. Boukhris, *J. Chem. Pharm. Res*. **2012**, 4, 5056.
[17] H. Zarrok, H. Oudda, A. El Midaoui, A. Zarrouk, B. Hammouti, M. Ebn Touhami, A. Attayibat, S. Radi, R. Touzani, *Res. Chem. Intermed*. **2012**, 38, 2051.
[18] A. Ghazoui, A. Zarrouk, N. Bencaht, R. Salghi, M. Assouag, M. El Hezzat, A. Guenbour, B. Hammouti, *J. Chem. Pharm. Res*. **2014**, 6, 704.
[19] H. Zarrok, A. Zarrouk, R. Salghi, M. Ebn Touhami, H. Oudda, B. Hammouti, R. Touir, F. Bentiss, S.S. Al-Deyab, *Int. J. Electrochem. Sci*. **2013**, 8, 6014.
[20] A. Zarrouk, H. Zarrok, R. Salghi, R. Touir, B. Hammouti, N. Benchat, L.L. Afrine, H. Hannache, M. El Hezzat, M. Bouachrine, *J. Chem. Pharm. Res*. **2013**, 5, 1482.
[21] H. Zarrok, A. Zarrouk, R. Salghi, M. Assouag, B. Hammouti, H. Oudda, S. Boukhris, S.S. Al Deyab, I. Warad, *Der Pharm. Lett*. **2013**, 5, 43.
[22] D. Ben Hmamou, M.R. Aouad, R. Salghi, A. Zarrouk, M. Assouag, O. Benali, M. Messali , H. Zarrok, B. Hammouti, *J. Chem. Pharm. Res*. **2012**, 4, 3498.
[23] M. Belayachi, H. Serrar, H. Zarrok, A. El Assyry, A. Zarrouk, H. Oudda, S. Boukhris, B. Hammouti, Eno E. Ebenso, A. Geunbour, *Int. J. Electrochem. Sci*. **2015**, 10, 3010.
[24] H. Tayebi, H. Bourazmi, B. Himmi, A. El Assyry, Y. Ramli, A. Zarrouk, A. Geunbour, B. Hammouti, Eno E.Ebenso, *Der Pharm. Lett*. **2014**, 6(6), 20.
[25] H. Tayebi, H. Bourazmi, B. Himmi, A. El Assyry, Y. Ramli, A. Zarrouk, A. Geunbour, B. Hammouti, *Der Pharm. Chem*. **2014**, 6(5), 220.
[26] C., Varalakshmi, B.V., Appa Rao, *Anti_Corros. Methods Mater.*, **2001**, 48, 171.
[27] F. Bentiss, M. Traisnel, M. Lagrenee, *Corros. Sci.*, **2002**, 42, 127.
[28] M.N. Desai, M.B. Desia, C.B. Shah, S.M., Desia, *Corros. Sci.*, **1986**, 26, 827.
[29] H. Shokry, M. Yuasa, M. Sekine, R.M. Issa, H.Y. El-Baradie, G.K. Gomma, *Corros. Sci.*, **1998**, 40, 2173.
[30] M. Hosseini, F.L. Mertens Stijn, M. Ghorbani, M.R. Arshdi, *Mater. Chem. Phys.*, **2003**, 7, 8800.
[31] F. Baghaei Ravari, A. Dadgarinezhad, I. Shekhs hoaei, *Science*, **2009**, 22, 175.
[32] ASTM, G 31-72, American Society for Testing and Materials, Philadelphia, PA, **1990**.
[33] N. S. Patel, S. Jauhari, and G. N. Mehta, *Acta Chim. Slov.* **2010**, 57, 297.
[34] B. Hammouti, A. Zarrouk, S.S. Al-Deyab And I. Warad, *Orient. J. Chem.*, **2011**, 27, 23.
[35] L. Larabi, O. Benali, Y. Harek, *Mater. Lett*., **2007**, 61, 3287.
[36] T. Szauer, A. Brandt, *Electrochim. Acta*, **1981**, 26, 1253.
[37] N. M.Guan, L.Xueming, L. Fei, *Mater. Chem. Phys*. **2004**, *86*, 59.
[38] B. Ateya, B. E. El-Anadouli, F. M. El-Nizamy, *Corros. Sci.* **1984**, *24*, 509.

[39] I.B. Obot, N.O, Obi-Egbedi, *Corros. Sci.*, **2010**, 52, 198.
[40] K. Mallaiyaa, R. Subramaniama, S.S. Srikandana, S. Gowria, N. Rajasekaranb, A. Selvaraj, *Electrochim. Acta*, **2011**, 56, 3857.
[41] E.S. Ferreira, C. Giacomelli, F.C. Giacomelli, A. Spinelli, *Mater. Chem. Phys.* **2004**, 83, 129.
[42] A.O. Yuce, G. Kardas, *Corros. Sci.* **2012**, 58, 86.
[43] D. A. L´opez, S. N. Simison and S. R. de S´anchez, *Electrochim. Acta*, **2003**, 48, 845.
[44] S. A. Umoren, Y. Li and F. H. Wang, *Corros. Sci.*, **2010**, 52, 2422.
[45] X.H. Li, S.D. Deng, H. Fu, *Corros. Sci*. **2011**, 53, 302.
[46] K.R. Ansari, M.A. Quraishi, A. Singh, *Corros. Sci*. **2014**, 79, 5.
[47] M.A. Amin, M.M. Ibrahim, *Corros. Sci*. **2011**, 53, 873.
[48] S.A. Umoren, Y. Li, F.H. Wang, *Corros. Sci*. **2010**, 52, 1777.
[49] D.K. Yadav, M.A. Quraishi, B. Maiti, *Corros. Sci*. **2012**, 55, 254.
[50] N.D. Nam, Q.V. Bui, M. Mathesh, M.Y.J. Tan, M. Forsyth, *Corros. Sci*. **2013**, 76, 257.
[51] A. Kosari, M.H. Moayed, A. Davoodi, R. Parvizi, M. Momeni, H. Eshghi, H. Moradi, *Corros. Sci*. **2014**, 78, 138.
[52] S. A. Umoren, Y. Li and F. H. Wang, *Corros. Sci*. **2010**, 52, 1777.
[53] A. K. Singh and M. A. Quraishi, *Corros. Sci*. **2010**, 52, 152.